

Solvent Dynamics in Aqueous PEO–Salt Solutions studied by Nuclear Magnetic Relaxation

Jan Breen, Dolf Huis, Jan de Bleijser and Jaap C. Leyte*

*Gorlaeus Laboratories, Department of Physical and Macromolecular Chemistry,
Leiden University, P.O. Box 9502, RA Leiden, The Netherlands*

The dynamical behaviour of water in aqueous PEO solutions has been studied by ^2H and ^{17}O nuclear magnetic relaxation measurements. A two-phase model is introduced to analyse the water mobility in the PEO hydration phase. The water mobility in the hydrated phase is retarded by a factor of 2 to 5. The anisotropic reorientation of water molecules in the proximity of PEO and the d_p -dependence on the ^2H and ^{17}O relaxation rates are interpreted qualitatively by local PEO dynamics, preferential orientations of water molecules and deuteron exchange among water molecules and hydroxy end-groups.

Nuclear magnetic relaxation measurements provide information about the dynamic behaviour of nuclei in solution. One of the topics in n.m.r. is the study of solvent–solute interactions. A lot of work has been focussed on biological systems, *e.g.* water–protein interactions have been investigated by ^1H , ^2H and ^{17}O water n.m.r.¹ The complexity of biological molecules excludes a simple physical interpretation of the results. More fundamental studies of water–solute interactions may be performed using silica or synthetic polymers.

For low solute concentrations, the water–solute interactions often result in small effects on the relaxation of solvent nuclei as a result of the low number of solute interaction sites and the low degree of interaction. In terms of a two-phase model, the fraction of bound water is small compared to the fraction of free water and the bound-water mobility is only slightly influenced in dilute solutions. To investigate the water–solute interaction more extensively, a large concentration range has to be examined. However, in concentrated solutions, the solvent–solute interactions may change: a number of solute interaction sites may be screened by the increase in solute–solute interactions, the water translational diffusion will decrease and the fraction of free water diminishes and may vanish ultimately in very concentrated solutions.

Aqueous poly(ethylene oxide) solutions were studied to obtain insight in the hydration properties of an uncharged polymer. The existence of dipole moments in the backbone, together with the intrinsic flexibility and the low thermal stability of the solid lattice (m.p. $\approx 60^\circ\text{C}$) result in the excellent solubility of PEO in water.² Because of the complete miscibility of PEO and water, this system can be used to study the water–solute interaction over a large concentration range.

Thermodynamic studies show a negative excess entropy and a negative interchange energy for the water–PEO interaction.^{2–6} This is interpreted by water structures around PEO and hydrogen bonding is suggested. No indications were obtained for the existence of ordered PEO structures in water. An analogous conclusion was formulated from a microcalorimetric study of PEO in water and in a water–ethanol mixture.⁷ Large, ordered PEO structures would not be in agreement with a previous n.m.r. study, in which short-range correlations ($\leq 1\text{ nm}$) were found to dominate.⁸

For a quantitative analysis of the experimental data, the number of water molecules interacting with one ethylene oxide group has to be known. Hydration and bulk water

properties can only be measured separately in few cases. If the exchange rate between bound and bulk phases is fast with respect to the relaxation rates, an average rate is observed in n.m.r. Introducing hydration and bulk water fractions then leads to the hydration water properties if the bulk is assumed invariant. The hydration water fraction will be proportional to the hydration number per ethylene oxide group.

The hydration number per monomeric unit has been evaluated from a number of experiments: adiabatic compressibility, evaporation, water diffusion, chemical shift, dielectric and melting studies.^{9–13} The decrease in adiabatic compressibility is related to the existence of bound water molecules, whereas the change in the dielectric constant as function of the frequency is related to the reorientational time of hydrated water molecules and the number of hydrated water molecules.^{9,13} A sudden transition is observed as a function of the PEO concentration in the chemical shift of water and ethylene protons, the water diffusion coefficient and the melting behaviour. The concentration at which this occurs is associated with the hydration number of the EO group.^{9–12} Frequently a hydration number of two is found, but melting and dielectric studies yield other hydration numbers. From the melting behaviour of PEO solutions two hydration numbers are derived, 1.6 and 3.7.¹² A hydration number of 5–6 is obtained from the dielectric measurements in 1 mol kg^{−1} solutions.¹³

The hydration number of 2 is interpreted by hydrogen bonding of two water molecules with the ether oxygen,⁶ however, in dilute aqueous PEO solutions, both the ether oxygen and the ethylene group will be surrounded by water molecules. A structural model of the PEO–water interactions in dilute solution, in which the number of hydrogen bonds among water molecules and between water and ether oxygen atoms is maximized, shows an enhanced water structure around PEO. The number of water molecules involved in hydrogen bonding between two ether oxygen atoms is 5.¹⁴

In this report the dynamical behaviour of water is studied by ²H and ¹⁷O nuclear magnetic relaxation. The relaxation rates are presented as a function of the PEO concentration and d_p . In order to study the ion relaxation, a small amount of salt was added (0.1 mol kg^{−1} salt). The influence of this addition on the water relaxation rates is negligible at room temperature. The ions used here have a moderate interaction with the water molecules, and the ion–PEO interaction is even less important in aqueous solutions.^{15, 16}

Theory

Water Dynamics

The water dynamics can be investigated by ¹H, ²H and ¹⁷O n.m.r. In strongly ordered liquids, the observed line splitting provides information about the water reorientation.¹⁷ For less ordered samples, the dipolar and quadrupolar interaction tensors are averaged within the relaxation time and no line splitting is observed, but the water dynamics can still be studied by nuclear magnetic relaxation. As a consequence of the different orientation of the interaction tensors in the molecular frame, the ratios of ¹H, ²H and ¹⁷O relaxation rates contain information about the water reorientation. For quadrupolar relaxation the interaction tensor is represented by the electric field gradients V_{xx} , V_{yy} and V_{zz} . The orientation of the principal axes of the interaction tensors for ²H and ¹⁷O is shown in fig. 1.^{18, 19}

The proton dipolar induced relaxation is complicated because both the intermolecular and the intramolecular relaxation mechanisms contribute to it. In concentrated PEO solutions, cross-relaxation between PEO and water protons may occur.²⁰ Hence the water proton relaxation will not be treated here.

The ²H and ¹⁷O quadrupolar relaxation mechanism is intramolecular, thus the rotational diffusion motion of a water molecule is examined by ²H and ¹⁷O n.m.r. The extreme narrowing conditions are satisfied for both water dynamics in the bulk phase

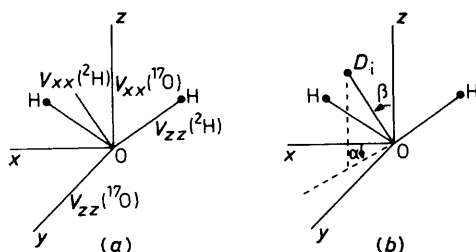


Fig. 1. (a) The principal axis of the field gradient tensor of ${}^2\text{H}$ and ${}^{17}\text{O}$. The water molecule is in the xz -plane. (b) The polar angles describing the orientation of the D_i axis relative to the molecular frame x, y, z and indicated by α, β .

and water dynamics in the hydration phase of PEO. In consequence, the relation for the quadrupolar relaxation becomes:

$$R_1 = R_2 = \frac{3}{80} \frac{2I+3}{I^2(2I-1)} \left(\frac{e^2 q Q}{\hbar} \right)^2 \left(1 + \frac{\eta^2}{3} \right) \tilde{J}(0) \quad (1)$$

where I is the spin quantum number, $e^2 q Q / \hbar$ is the quadrupole coupling constant, η is the asymmetry parameter [$\eta = -(V_{xx} - V_{yy}) / V_{zz}$] and $\tilde{J}(0)$ is the reduced spectral density defined by

$$\tilde{J}(0) = \frac{1}{G(0)} \int_{-\infty}^{\infty} G(t) dt. \quad (2)$$

The correlation function $G(t)$ describes the time-dependent correlation of the electric field gradient tensor components. The electric field gradient tensor components are represented by functions $B_m^{(2)}$, which transform as second-rank spherical harmonics. A transformation is performed by Wigner matrices. The transformation from the laboratory frame to the diffusion frame is represented by the angle Ω :

$$G_m(t) = \langle B_m^{(2)}(0) B_m^{(2)*}(t) \rangle_{\text{lab}} = \sum_{k,n} B_k^{(2)'} B_n^{(2)'} \langle D_{km}^{(2)}[\Omega(0)] D_{nm}^{(2)*}[\Omega(t)] \rangle. \quad (3)$$

The transformation to the interaction frame leads to

$$G_m(t) = \sum_{k,l,n,p} B_l^{(2)''} B_p^{(2)''*} D_{lk}^{(2)}(\Omega') D_{pn}^{(2)*}(\Omega') \langle D_{km}^{(2)}[\Omega(0)] D_{nm}^{(2)*}[\Omega(t)] \rangle. \quad (4)$$

The latter transformation, represented by the angle Ω' , is time-independent. The $B^{(2)''}$ components are characterized by

$$B_0^{(2)''} = \sqrt{3/2}, B_{\pm 1}^{(2)''} = 0 \quad \text{and} \quad B_{\pm 2}^{(2)''} = \eta/2.$$

The laboratory \rightarrow diffusion transformation is determined by the reorientation behaviour of the water molecule.

In case of an overall rotational diffusion and an internal diffusion along one axis the correlation function $G(t)$ becomes

$$G_m(t) = \sum_{k,l,p} B_l^{(2)''} B_p^{(2)''*} D_{lk}^{(2)}(\Omega') D_{pk}^{(2)*}(\Omega') \exp[-(6D_0 + k^2 D_i) t] \quad (5)$$

resulting in the correlation times

$$\tau_0 = (6D_0)^{-1}, \quad \tau_1 = (6D_0 + D_i)^{-1} \quad \text{and} \quad \tau_2 = (6D_0 + 4D_i)^{-1}. \quad (6)$$

The coefficients associated with the different correlation times are different for ${}^2\text{H}$ and ${}^{17}\text{O}$ as a result of $\Omega'({}^2\text{H}) \neq \Omega'({}^{17}\text{O})$. The angle Ω' , representing the orientation of the interaction frame relative to the diffusion frame, is not easily visualized. In consequence

the orientation of the diffusion axis is represented by the angles α and β as shown in fig. 1.

The model, overall rotation with internal rotation about one axis, is mathematically equivalent to an anisotropic reorientational model, in which axial symmetry is assumed. This anisotropic reorientation is described by two diffusion coefficients D_{\parallel} and D_{\perp} . By substituting $D_0 \rightarrow D_{\perp}$ and $D_i \rightarrow D_{\parallel} - D_{\perp}$ in eqn (5) and (6), the correlation times and associated coefficients for the anisotropic reorientational model are obtained.

The ^2H and ^{17}O relaxation data will be examined using the simple models discussed above. Other more detailed models cannot be tested owing to the fact that no information is obtained from field-dependent measurements because $\omega\tau_i \ll 1$. Only one average ^2H correlation time and one average ^{17}O correlation time are obtained in a given PEO sample.

Model

A two-phase model is used to analyse the nuclear magnetic relaxation data. Two regions, a free phase and a PEO hydration phase, are introduced. The free phase is characterized by the pure solvent properties, whereas the hydration phase contains the solvent molecules disturbed by PEO. The phase boundaries are related to the solute–solvent interaction potential. However, the exact interaction potential is unknown. Only simplified models and computer simulations concerning solute–solvent interactions have been published.^{21–23} It is concluded that the solute–solvent interaction is short-range. This conclusion is in agreement with the results of an n.m.r. investigation in which the proton and deuteron relaxation rates were studied as a function of the distance between clay sheets.²⁴

The relaxation rate in a two-phase model, in which the exchange between the two phases is fast compared to the relaxation rates and slow compared to the correlation times, is given by:

$$R_{\text{exp}} = PR_{\text{h}} + (1 - P)R_{\text{f}} \quad (7)$$

where R_{exp} is the experimental relaxation rate, R_{h} is the relaxation rate in the hydration layer around PEO and R_{f} is the relaxation rate in the free phase.

The applicability of eqn (7) is limited to dilute polymer solutions. For dilute solutions, it turns out that the results to be reported in subsequent sections are consistent with constant values for R_{h} and R_{f} in combination with a proportional relation of P and the polymer concentration. In concentrated solutions, P will not be proportional to the solute concentration as a result of increased polymer–polymer contacts and associated screening of polymer sites for solvent contact. The increased polymer contacts diminish the polymer segment mobility. In consequence the water mobility in the hydration phase will be reduced. Both P and R_{h} will depend on the polymer concentration. The expression for P is:

$$P = \frac{n(c)c}{55.5} \quad (8)$$

where c is the polymer concentration in mol kg^{-1} solvent and n is the hydration number. Substituting into eqn (7) gives

$$R_{\text{exp}} - R_{\text{f}} = \frac{n(c)c}{55.5} [R_{\text{h}}(c) - R_{\text{f}}]. \quad (9)$$

Although the results to be discussed are consistent with a constant hydration number below a critical concentration (*ca.* 5 mol kg^{-1}), this invariance cannot be verified directly. As a consequence R_{h} cannot be calculated from the experimental ^2H and ^{17}O relaxation rates. The hydration numbers presented in the previous section yield an estimate of the range of R_{h} and the correlation time in the hydrated layer of PEO.

Table 1. Characterization of PEO samples

sample		\bar{M}_n	d_p
PEO 200	(Merck)	$(1.9 \pm 0.1) \times 10^2^a$	4
PEO 400	(Merck)	$(3.9 \pm 0.2) \times 10^2^a$	9
PEO 1000	(Merck)	$(9.5 \pm 0.5) \times 10^2^a$	22
PEO 4000	(Merck)	$(3.7 \pm 0.2) \times 10^3^a$	84
PEO 20000	(Merck)	$(1.6 \pm 0.1) \times 10^4^b$	360
PEO 20000	(Fluka)	$(1.3 \pm 0.1) \times 10^4^b$	300
SE-8	(Toya Soda)	$7.8 \times 10^4^c$	1800
PEO 300 000	(Poly Science)	$(1.2 \pm 0.2) \times 10^5^b$	2700

^a Vapour pressure. ^b Membrane osmotic pressure. ^c Value given by manufacturer.

Experimental

Materials

The different PEO fractions used in this study are given in table 1. Characterizations were performed on a Hitachi vapour-pressure osmometer, a Knauer membrane osmometer, a KMX-6 (low-angle laser light scattering) and a Scott viscometer. The PEO samples were used without purification, except the Poly Science product. The aqueous solutions of the original Poly Science product were cloudy and alkaline, therefore this sample was purified by filtration and dialysis.⁸

The PEO solutions were prepared by weight, using an aqueous salt solution as solvent. The salt solution was enriched with ²H (0.2 % w/w) and with ¹⁷O (0.1 % w/w). The PEO solutions were degassed in a vacuum desiccator, after which they were stored in N₂ or Ar atmosphere at 4 °C to prevent degradation of PEO. Some of the more concentrated solutions were obtained by evaporation of the solvent.

The salts used were of the highest purity commercially available. The enriched ²H- and ¹⁷O-water was obtained from the Monsanto Research Corporation.

Nuclear Magnetic Relaxation Experiments

The n.m.r. experiments were performed on a pulse spectrometer (home-built) at a field of 6.3 T (Oxford Instruments superconducting magnet). The temperature was maintained at 25 ± 1 °C by a Bruker VT 1000 air thermostat. The longitudinal relaxation rates were obtained from inversion recovery experiments, whereas the transverse relaxation rates were obtained from spin-echo or Carr–Purcell–Gill–Meiboom pulse sequence experiments. A number of transverse relaxation rates were determined throughout the concentration range studied in order to check the equality of R_1 and R_2 or to study the deuteron exchange.

Results and Discussion

Water Dynamics

The relative ²H and ¹⁷O longitudinal relaxation rates *vs.* the PEO concentration are shown in fig. 2 for PEO 200 ($d_p = 4$) and PEO 400 ($d_p = 9$) and in fig. 3 for PEO 20000 ($d_p = 300$ and 360) and PEO 300 000 ($d_p = 2700$). It is observed that the relative ¹⁷O relaxation rate exceeds the relative ²H relaxation rate for the higher molecular weights. For PEO 200 the relative ²H relaxation is somewhat larger. This phenomenon will be

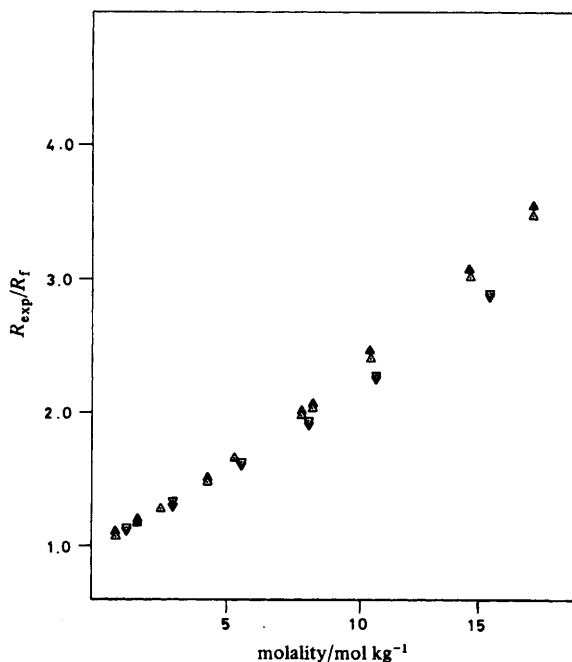


Fig. 2. The relative ^2H and ^{17}O relaxation rates *vs.* the PEO concentration at 25 °C: ∇ , ^2H ; \blacktriangledown , ^{17}O ; PEG 200 ($d_p = 4$); 0.1 mol kg⁻¹ NaCl. \triangle , ^2H ; \blacktriangle , ^{17}O ; PEG 400 ($d_p = 9$); 0.1 mol kg⁻¹ NaBr.

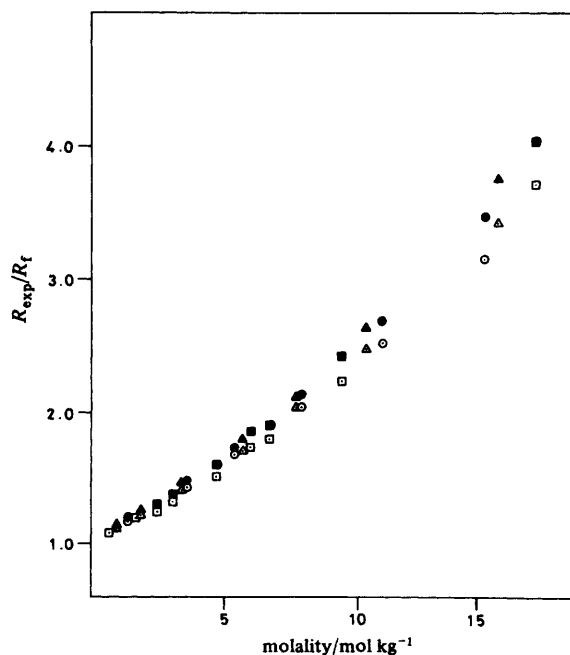


Fig. 3. The relative ^2H and ^{17}O relaxation rates *vs.* the PEO concentration at 25 °C: \circ , ^2H ; \bullet , ^{17}O ; PEG 20000 ($d_p = 360$); 0.1 mol kg⁻¹ CsCl. \triangle , ^2H ; \blacktriangle , ^{17}O ; PEG 20000 ($d_p = 300$); 0.1 mol kg⁻¹ NaBr. \square , ^2H ; \blacksquare , ^{17}O ; PEG 300000 ($d_p = 2700$); 0.1 mol kg⁻¹ NaBr.

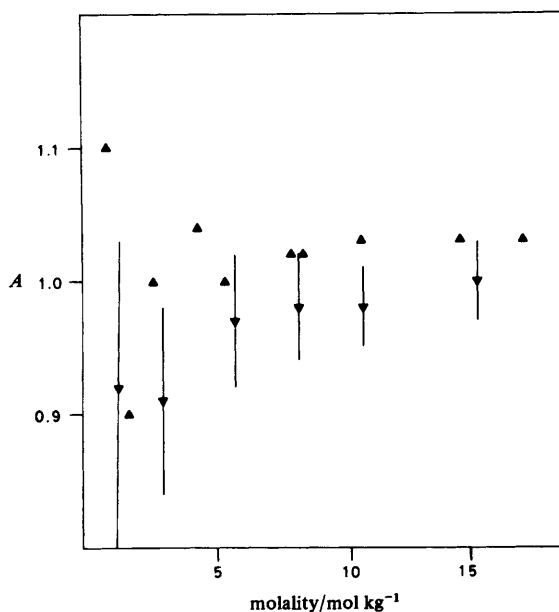


Fig. 4. The ratio A , defined by eqn (10), plotted as a function of the PEO concentration: ▼, PEG 200 ($d_p = 4$); ▲, PEG 400 ($d_p = 9$).

discussed in the next section. Further, the onset of curvature is noted in the data presented in fig. 2 and 3.

The relative enhancement of the ^2H and ^{17}O relaxation rates may be expressed by the ratio

$$A = \frac{R_{\text{exp}}(^{17}\text{O}) - R_r(^{17}\text{O})}{R_{\text{exp}}(^2\text{H}) - R_r(^2\text{H})} \frac{R_r(^2\text{H})}{R_r(^{17}\text{O})} = \frac{R_h(^{17}\text{O}) - R_r(^{17}\text{O})}{R_h(^2\text{H}) - R_r(^2\text{H})} \frac{R_r(^2\text{H})}{R_r(^{17}\text{O})}. \quad (10)$$

Although A is not equal to the ratio of the relative ^2H and ^{17}O relaxation rates, it may serve to identify the anisotropic reorientation of the water molecule in the hydration phase of PEO. The ratio of the experimental ^2H and ^{17}O relaxation rates disguises the anisotropic reorientation, whereas the A emphasizes this phenomenon. The A values corresponding to the relaxation data in fig. 2 are given in fig. 4 and the A values corresponding to the relaxation data in fig. 3 are given in fig. 5. The experimental error is largest for the less concentrated solutions, in which $R_{\text{exp}} \approx R_r$. The weighted average of the A values of fig. 5 is 1.12. A linear least-squares fit of these data results in:

$$A = (1.09 \pm 0.01) + (0.004 \pm 0.001) c. \quad (11)$$

The relative ^2H and ^{17}O relaxation rates are unequal, indicating an anisotropic reorientation of the hydrated water molecule even in dilute solutions. Anisotropic rotational diffusion of water molecules may indicate preferential orientation of water near PEO.

The water correlation time in the bound phase can be evaluated using the following coupling constants and asymmetry parameters for ^2H and ^{17}O .¹⁶

$$\begin{aligned} ^2\text{H}: \frac{eq^2Q}{h} &= 252 \text{ kHz}, \quad \eta = 0.135 \\ ^{17}\text{O}: \frac{eq^2Q}{h} &= 8.0 \text{ MHz}, \quad \eta = 0.75. \end{aligned} \quad (12)$$

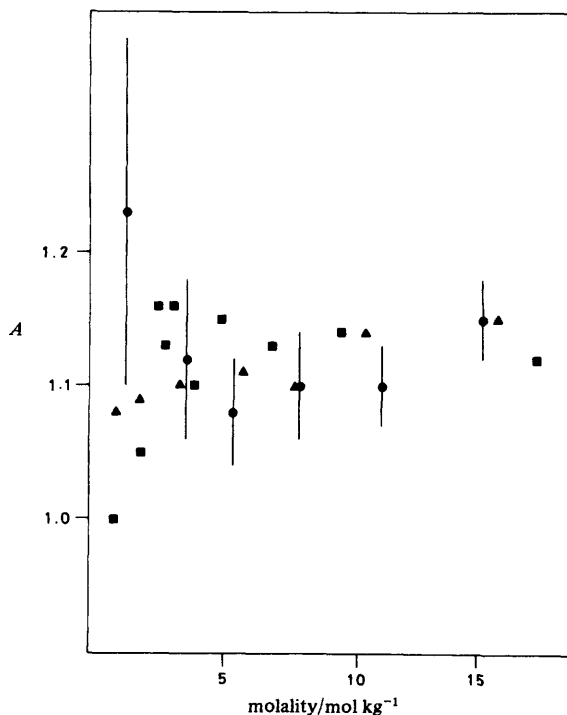


Fig. 5. The ratio A , defined by eqn (10), as function of the PEO concentration: ●, PEG 20000 ($d_p = 360$); ▲, PEG 20000 ($d_p = 300$); ■, PEO 300000 ($d_p = 2700$).

The coupling constants are calculated from the experimental relaxation rates in pure water using eqn (1). The gas values are used for the asymmetry parameters, $\eta(^2\text{H}) = 0.135$ and $\eta(^{17}\text{O}) = 0.75$. The correlation time, describing the isotropic rotational diffusion of a water molecule, is calculated from the dipolar ^1H – ^{17}O contribution to the ^1H relaxation rate using $r_{\text{OH}} = 0.098$ nm. It is assumed that the coupling constants are not influenced by the presence of PEO. An isotropic correlation time of 2.0 ps is then obtained for the dilute salt solutions used as solvent. This value is in agreement with the value of 1.95 ps found for the pure water solution, indicating the small influence of the ions.¹⁶ Studying the relative relaxation rates then yields

$$\frac{R_h}{R_t} = \frac{\tau_h}{\tau_t} = \frac{1}{2.0} \tau_h \quad (13)$$

where τ_h is given in ps. For the solutions with $c < 5$ mol kg^{−1} solvent in fig. 3, the slope of the relative relaxation rate *vs.* the PEO concentration is obtained from a least-squares fit. The slope for ^2H is 0.115 ± 0.007 and for ^{17}O is 0.128 ± 0.007 . Although the deviation in the slope is large due to the experimental error, the difference between ^2H and ^{17}O is clearly present. The relaxation rate in the hydrated phase around PEO, R_h , can be calculated from the slope S :

$$S = \frac{n}{55.5} \left(\frac{R_h}{R_t} - 1 \right). \quad (14)$$

Using a mean slope of 0.12 and substituting $n = 6$ leads to $\tau_h = 4.1 \pm 0.1$ ps. In the case of $n = 2$, $\tau_h = 8.4 \pm 0.2$ ps. The correlation time for hydration water molecules is therefore increased by a factor of 2 to 4 depending on the actual hydration number. The

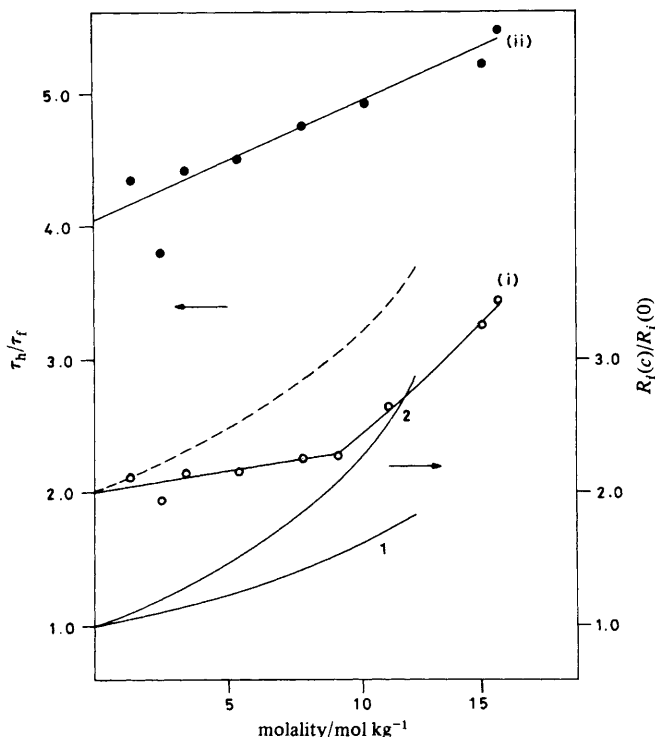


Fig. 6. The relative polymer ^1H relaxation rates for PEO 20000 ($d_p = 360$) as function of the PEO concentration. Relative longitudinal relaxation rates are given by line 1, whereas the relative transverse relaxation rates are given by line 2.⁸ The ratio τ_h/τ_f calculated from the ^2H solvent relaxation rates is given for (i) $n = 6$ for $c < 9.25 \text{ mol kg}^{-1}$ and $n = 55.5/c$ for $c > 9.25 \text{ mol kg}^{-1}$; (ii) $n = 2$. Some experimental data are shown (\circ , \bullet). The dashed line shows the ^1H PEO longitudinal relaxation scaled to τ_h/τ_f at zero polymer concentration.

factor of 2 is in agreement with the dielectric measurements of Kaatze *et al.*,¹³ in which a hydration number of 5 to 6 and $\tau_h/\tau_f = 2.2 \pm 0.2$ was estimated.

τ_h increases with PEO concentration and the size of the increase is dependent on the hydration number, as can be noted from fig. 6 in which two cases are considered: (i) $n = 6$ in the concentration range $0\text{--}9.25 \text{ mol kg}^{-1}$ solvent and $n = 55.5/c$ in the more concentrated solutions; (ii) $n = 2$. The actual hydration number will probably lie between those two values.

The relative correlation times τ_h/τ_f of ^2H are calculated for the PEO 20000 (degree of polymerization, $d_p = 300$ and 360) and PEO 300000 ($d_p = 2700$) samples using eqn (9) and (13). The concentration dependence of n in case (i) occurs because all water molecules are hydrated for PEO concentrations $> 9.25 \text{ mol kg}^{-1}$.

The correlation time of water in the PEO hydration shell may be influenced by the local polymer dynamics. The local polymer mobility as a function of the PEO concentration may be studied from the ^1H PEO relaxation rates.⁸ The results for τ_h/τ_f together with the relative ^1H PEO relaxation rates are shown as a function of the PEO concentration in fig. 6. The relative increase of τ_h/τ_f for $n = 2$ is smaller than the relative increase of the ^1H PEO relaxation rates. The longitudinal ^1H PEO relaxation rate is largely determined by the fast internal motion of PEO. The scaling of τ_h relative to R_1 (^1H PEO), assuming $n = 6$ for dilute PEO solutions, leads to the dashed line in fig. 6. This line is in between the solutions for (i) and (ii); however, now n is a function of the

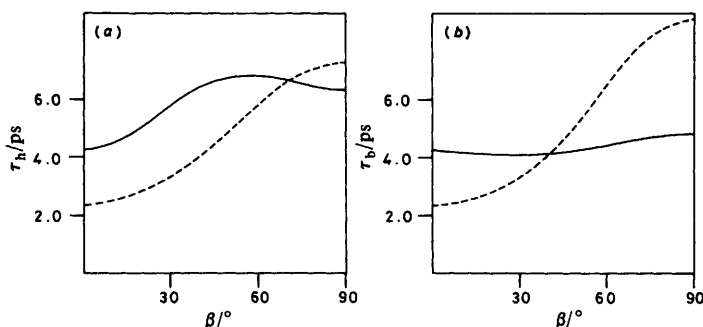


Fig. 7. The correlation time τ_h as a function of the angle β for $D_i = 8.0 \times 10^{10} \text{ s}^{-1}$ and $D_i/D_0 = 5$. (a) $\alpha = 0^\circ$, (b) $\alpha = 90^\circ$. The dashed line represents τ_h (^{17}O), whereas the solid line represents τ_h (^2H).

concentration (e.g. $n = 6$, for $c \approx 0$ and $n = 4$ for $c \approx 10 \text{ mol kg}^{-1}$ solvent). It is improbable that τ_h should scale exactly as $R_1(^1\text{H PEO})$, because τ_h is not only affected by the water–polymer interactions but also by water–water interactions and exchange processes; however, the scaling may indicate the trend in τ_h as a function of the PEO concentration.

Additional information can be obtained from the difference between the relative ^{17}O and the ^2H relaxation rates in the polymer solutions. From the correlation function $G(t)$ given in eqn (5) the following expression for τ_h is simply derived:

$$\tau_h = \sum_i a_i (\Omega') \tau_i$$

$$a_i = \frac{2}{3} \sum_{l,p} B_l^{(2)''} B_p^{(2)''*} D_{lk}^{(2)} (\Omega') D_{pk}^{(2)*} (\Omega') / \left(1 + \frac{\eta^2}{3}\right). \quad (15)$$

The coefficients a_i are calculated using the asymmetry parameters given in eqn (12) and $B_0^{(2)''} = \sqrt{3}/2$, $B_{\pm 1}^{(2)''} = 0$ and $B_{\pm 2}^{(2)''} = \eta/2$. As an example the correlation times τ_h for ^2H and ^{17}O when $D_i = 8.0 \times 10^{10} \text{ s}^{-1}$ and $D_i/D_0 = 5$ will be considered. For these values of the diffusion parameters, τ_h is evaluated as a function of the orientation of the diffusion tensor. The results are shown in fig. 7. Although the overall diffusion coefficient, D_0 , is smaller than the internal diffusion coefficient by a factor of 5, the correlation times for ^2H and ^{17}O differ at most by a factor of 2. The ^2H and ^{17}O relaxation rates are therefore not very sensitive for the anisotropy in the water mobility.

The physical interpretation of the reorientation model described by an overall and an internal motion may be binding of the water molecule to the PEO chain. Then the orientation of the internal diffusion axis may tentatively be identified with the orientation of the bond, and the overall diffusion coefficient may be identified with the diffusion coefficient representing the local PEO dynamics. However, the local PEO motion is not described by one diffusion coefficient.⁸ As a consequence the D_0 introduced is in this case an average diffusion coefficient and the orientation of the PEO–water bond will deviate from the orientation of the internal diffusion axis.

Instead of using the questioned concept of bound water molecules one might describe the molecular motion of the water molecules with an axially symmetric diffusion tensor with principal values D_{\parallel} and D_{\perp} . The anisotropic motion may then be thought to represent a less specified interference by PEO in the motional behaviour of the water molecules. Mathematically the two descriptions are equivalent, as D_{\perp} and D_{\parallel} are simply related to D_0 and D_i :

$$D_{\parallel} = D_0 + D_i \quad \text{and} \quad D_{\perp} = D_i. \quad (16)$$

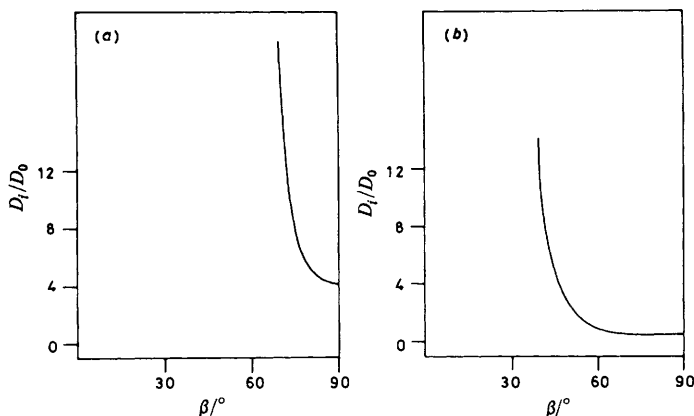


Fig. 8. The ratio D_i/D_0 as a function of the angle β for

$$\frac{R(^{17}\text{O}; c) R(^2\text{H}; 0)}{R(^{17}\text{O}; 0) R(^2\text{H}; c)} = 1.10$$

(a) $\alpha = 0^\circ$, (b) $\alpha = 90^\circ$.

The increase of relative ^{17}O relaxation rates as a function of the PEO concentration exceeds the ^2H relaxation rates. For PEO with sufficient large d_p the ratio given by eqn (10) is 1.10–1.14, depending on the concentration. Starting from $\tau_h(^{17}\text{O})/\tau_h(^2\text{H}) = 1.10$, possible orientations and associated D_i/D_0 ratios have been evaluated and are given in fig. 8. The orientation of the diffusion tensor is limited to the larger β values. Solutions for low β values are impossible, whereas the solutions for β values approaching 90° yield very low D_i/D_0 ratios. The solution for $\beta = 55^\circ$ and $\alpha = 0^\circ$ is outside the range of solutions found in fig. 8(a). As a consequence, pure hydrogen bonding is not probable.

A number of solutions can be excluded. Large D_i/D_0 ratios are not probable owing to the relatively fast local PEO motions.⁸ Further, D_i values larger than the isotropic diffusion coefficient obtained for pure water are not expected. If PEO–water binding occurs, the most probable solutions will be in the range $D_i/D_0 < 6$. The number 6 is an estimate for the case in which the bound water molecules experience an internal reorientation process comparable with the pure water dynamics (2 ps) and an overall reorientation process comparable with the fast polymer dynamics (12 ps).⁸ Low D_i/D_0 values may indicate an internal motion slow compared to the bulk water mobility. Evaluation of the diffusion coefficients for $\tau_h(^{17}\text{O})/\tau_h(^2\text{H}) = 1.10$ and $\tau_h(^{17}\text{O}) = 6$ ps yields D_i and D_0 values shown in fig. 9.

An arbitrary value for $\tau_h(^{17}\text{O})$ is chosen. The correlation time of 6 ps corresponds to a ratio $\tau_h/\tau_f = 3$. This value is in between the boundaries shown in fig. 6. The dashed line in fig. 9 represents the pure water diffusion coefficient. From fig. 8 and 9 it is concluded that possible preferential orientations of water molecules in the proximity of PEO are

$$\alpha = 0^\circ, \quad 80 < \beta/^\circ < 90$$

and

$$\alpha = 90^\circ, \quad 40 < \beta/^\circ < 90.$$

For intermediate α values, the β values will be in the range 40 – 90° . No specific orientation of the water molecule will be found for a number of reasons: *e.g.* the amphiphilic character of the PEO chain may result in a distribution of preferential water orientations and the water molecules in the proximity of PEO are not influenced by PEO only, but interact also with surrounding water molecules.

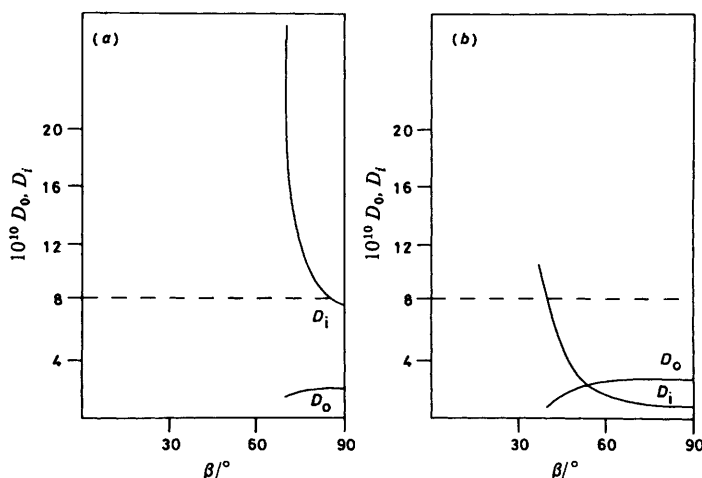


Fig. 9. The diffusion coefficients D_i and D_o calculated for $\tau_h(^{17}\text{O}) = 6$ ps and $\tau_h(^2\text{H}) = 5.45$ ps: (a) $\alpha = 0^\circ$, (b) $\alpha = 90^\circ$. The dashed line represents the pure water diffusion coefficient.

These results can also be compared to some related studies concerning the hydrophobic hydration of apolar solutes. The hydrophobic hydration has been investigated by molecular dynamics simulations for aqueous solutions containing two Lennard-Jones spheres. The molecular mobility of the solvent in the hydration layer is reduced by a factor of two at most. The lifetime of the hydrogen bond is longer in the solvation sphere compared to the bulk phase.²⁵ The preferential orientation of the water dipole relative to the Lennard-Jones water-sphere vector has also been evaluated. In the first shell, one of the four tetrahedral bonds (O—H and lone pairs) points radially outwards, resulting in the orientations $\alpha = 0$ or 90° and $\beta = 54.7^\circ$.²² An n.m.r. investigation by Hertz, in which the hydration of the methyl group of methanol was studied by comparing the relaxation contribution caused by ^{17}O with the contribution due to water protons, yields as possible orientations $\alpha = 0^\circ$ and $\beta = 56^\circ$ or $\alpha = 90^\circ$ and $\beta = 81^\circ$.²⁶ The hydration of PEO is more complicated owing to its amphiphilic character and local mobility. As a consequence the preferential orientation found for the PEO-hydrated water molecules will be an average. The preferential orientations obtained from the molecular dynamics simulations do not contradict the preferential orientation found here for water molecules in the proximity of PEO. Nevertheless the physical interpretation in terms of water-PEO binding should possibly not be carried to this level of detail. Interpretation of the water dynamics in the phase disturbed by PEO in terms of the general anisotropic reorientational diffusion model may be preferred. Using this model it is concluded that the average reorientation of water molecules in the PEO solvation sphere is slightly anisotropic and that D_{\parallel}/D_{\perp} is in the range 1–7.

Molecular Weight Dependence

The molecular weight dependence of ^2H and ^{17}O relaxation rates reflects the less restricted segment mobility in short polymers.⁸ The polymer segment dynamics are related to the ^1H PEO relaxation rates. The ratio

$$\frac{R_1(^1\text{H}, d_p = 9)}{R_1(^1\text{H}, d_p = 360)} = 0.69 \quad (17)$$

indicating faster polymer dynamics (shorter correlation times) for PEO ($d_p = 9$), is much smaller than the ratio

$$\frac{R_{\text{exp}}(^{17}\text{O}; d_p = 9) - R_f(^{17}\text{O}; d_p = 9)}{R_{\text{exp}}(^{17}\text{O}; d_p = 360) - R_f(^{17}\text{O}; d_p = 360)} = 0.92 \quad (18)$$

obtained from the slopes for ^{17}O , $c < 5$ mol kg^{-1} solvent. The reduction of the water mobility in the PEO hydration sphere is less affected by the degree of polymerization than the ^1H local PEO dynamics. Although the trend is the same, the correlation time, τ_h , is not exclusively determined by the polymer dynamics.

Another interesting feature is the behaviour of the ^2H and the ^{17}O relative relaxation rates for short chains (fig. 2). Almost no difference in the relative ^2H and ^{17}O relaxation rates is observed, suggesting a lower anisotropy in the water reorientation. The average ratio A , defined in eqn (10) and representing the anisotropy of the water motion, can be calculated for the PEG 200 and PEG 400 solutions using the values presented in fig. 4: PEG 200 ($d_p = 4$): $\bar{A} = 0.97$ and PEG 400 ($d_p = 9$): $\bar{A} = 1.02$. However, another phenomenon becomes important for low d_p , the exchange of deuterons between water and the hydroxy end-groups. The number of hydroxy end-groups is proportional to d_p^{-1} .

Only one longitudinal ^2H relaxation rate is observed, indicating fast exchange between the two deuteron sites. In consequence, the longitudinal ^2H relaxation rate is the weighted average of the relaxation rate in the different sites. Because the ^2H relaxation rate in the PEO hydroxy end-group will be larger than that in the hydrated water molecule, the ratio of ^{17}O and ^2H relaxation rates diminishes. Thus the contribution of deuterons in the hydroxy end-group to the ^2H longitudinal relaxation rate decreases the A value for low-molecular-weight PEG samples.

The exchange contribution to the transverse ^2H relaxation rate can be studied by spacing-dependent Carr–Purcell–Gill–Meiboom experiments.^{27,28} The deuterons of water and the PEO hydroxy group are in different chemical environments. The deuteron relaxation rate in the PEO end-group will be of the same order of magnitude as the water deuteron relaxation rate. The correlation time for the PEO deuterons, estimated from the ^{13}C relaxation rates of the end-groups,⁸ will be *ca.* 7 ps. The quadrupole coupling constant is not expected to change much because the OH distance in methanol almost equals the OH distance in water. Further, the scalar coupling with ^{17}O is negligible due to the low amount of ^{17}O (*ca.* 0.1 %). Therefore the spacing dependence in R_2 is caused by the fact that the two deuteron sites have different Larmor frequencies, ω_A and ω_B . Because the exchange rate between the two deuteron sites is fast compared to the average relaxation rate, no influence of the exchange is observed in the longitudinal relaxation rate. However, as a result of the different Larmor frequencies, line-broadening is observed for the transverse relaxation process. The line-broadening, modulated by the exchange rate, can be diminished by a Carr–Purcell–Gill–Meiboom sequence if the pulse spacing between the two successive 180° pulses, τ_s , is smaller than the exchange time, τ_e . Thus the spacing dependence of the transverse ^2H relaxation rates yields an estimate of the exchange time and the frequency difference $\omega_A - \omega_B$.

The PEO 200 ($d_p = 4$) results are given in table 2. A useful approximation for the spin–spin relaxation rate as function of the spacing τ_s is:²⁷

$$R_2(\tau_s) = R_1 + p_A p_B (\omega_A - \omega_B)^2 \tau_e \left(1 - 2 \frac{\tau_e}{\tau_s} \tanh \frac{\tau_s}{2\tau_e} \right) \quad (19)$$

where $\tau_e^{-1} = \tau_A^{-1} + \tau_B^{-1}$ (the exchange time), $p_A = \tau_A / (\tau_A + \tau_B)$, $p_B = \tau_B / (\tau_A + \tau_B)$ and τ_A and τ_B are lifetimes. The indices A and B represent the different sites. The longitudinal relaxation rate R_1 is the average of the longitudinal relaxation rates R_{1A} and R_{1B} . In

Table 2. ^2H -Exchange studied by CPGM spacing-dependent experiments at 25 °C and 6.3 T

$c/\text{mol kg}^{-1}$	R_1/s^{-1}	$R_2(\tau_s)/\text{s}^{-1}$				
		$\tau_s = 1 \text{ ms}$	$\tau_s = 2 \text{ ms}$	$\tau_s = 3 \text{ ms}$	$\tau_s = 4 \text{ ms}$	$\tau_s = 6 \text{ ms}$
8.1	3.9 ± 0.1	—	4.3	4.6	—	4.8
10.5	4.5 ± 0.1	—	5.1	5.4	—	5.9
14.8	5.8 ± 0.1	6.1	6.5	—	7.1	—

order to check the relaxation mechanism, the spacing dependence of PEO 200 solutions was also studied at 2.1 T. The reduction in the spacing dependence of $R_2 - R_1$ at 2.1 T is in agreement with the frequency dependence given in eqn (19). Thus the chemical shift is responsible for the spacing dependence in R_2 .

A trial-and-error least-squares fit of the spacing-dependent R_2 value has been performed. An exchange time, $\tau_e = 0.8 \pm 0.2 \text{ ms}$, and frequency difference of $33 \pm 3 \text{ Hz}$ are obtained. Because the number of water deuterons is much larger than the number of hydroxy end-group deuterons, the exchange time equals the residence time of hydroxy end-group deuterons.

The exchange rate is pH-dependent. The PEO 200 solutions (table 2) have a pH of 5.6 ± 0.1 . Addition of HCl to the PEO 200 solutions reduces the spacing dependence. At pH 2, no difference in R_2 and R_1 is observed. This is analogous to the proton exchange in pure water. At pH 7 the exchange time is *ca.* 2 ms, whereas at pH 5.6 the exchange time is *ca.* 0.2 ms.²⁹

Conclusions

The ^2H and ^{17}O relaxation rates have been interpreted by a two-phase model. The correctness of the two-state model is doubtful in concentrated solutions, because then both the relaxation rate, R_n , and the hydration number, n , change. The relaxation rate in the bound phase is a factor of 2 to 5 larger than in pure water, indicating a retardation of the water dynamics. The difference between relative ^2H and ^{17}O relaxation is explained by anisotropic reorientation of the water molecules. The anisotropy is small as a result of the fast internal PEO motion. The anisotropy may indicate a preferential orientation of water molecules in the proximity of PEO; however, pure hydrogen bonding is not observed.

The molecular weight dependence of the ^2H and ^{17}O relaxation rates is caused by the molecular weight dependence in the local PEO dynamics and by deuteron exchange. The molecular weight dependence in the PEO segment mobility is a result of the less restricted polymer dynamics for short chains.

Extended ^2H and ^{17}O n.m.r. studies on the hydration of polymers are scarce. The presence of many hydroxy and carboxyl groups in polyacids and biological macromolecules yields contributions to the ^2H relaxation rate and complicates analysis of the data.³⁰ The ^{17}O relaxation rate is not influenced by this exchange and represents the water dynamics. Although the behaviour of the ^{17}O relaxation rate in PAA ($\alpha = 0$) solutions is comparable with the PEO data, the order of anisotropy cannot be checked.³¹

References

- 1 S. H. Koenig, K. Hallenga and M. Shporer, *Proc. Natl Acad. Sci. USA*, 1975, **72**, 2667.
- 2 F. E. Bailey and J. V. Koleske, *Polyethylene Oxide* (Academic Press, New York, 1976).
- 3 G. N. Malcolm and J. S. Rowlinson, *Trans. Faraday Soc.*, 1957, **53**, 921.
- 4 M. L. Lakhanpal, K. S. Chhina and S. C. Sharma, *Ind. J. Chem.*, 1968, **6**, 505.

- 5 E. A. Boucher and P. M. Hines, *J. Polym. Sci., Polym. Phys. Ed.*, 1978, **16**, 501.
- 6 R. Kjellander and E. Florin, *J. Chem. Soc., Faraday Trans. 1*, 1981, **77**, 2053.
- 7 H. Daoust and D. StCyr, *Macromolecules*, 1984, **17**, 596.
- 8 J. Breen, D. van Duijn, J. de Bleijser and J. C. Leyte, *Ber. Bunsenges. Phys. Chem.*, 1986, **90**, 1112.
- 9 B. P. Makogon and T. A. Bondarenko, *Vysokomol. Soedin A*, 1985, **27**, 563.
- 10 K. J. Liu and J. L. Parsons, *Macromolecules*, 1969, **2**, 529.
- 11 V. D. Zinchenko, V. V. Mank, V. A. Moiseev and F. D. Ovcharenko, *Kolloidn. Zh.*, 1976, **39**, 30.
- 12 B. Bogdanov and M. Mihailov, *J. Polym. Sci., Polym. Phys. Ed.*, 1985, **23**, 2149.
- 13 U. Kaatz, O. Gottman, R. Podbielski, R. Pottel and U. Terveer, *J. Phys. Chem.*, 1978, **82**, 112.
- 14 A. I. Toryanik, *Zh. Strukt. Khim.*, 1984, **25**, 49.
- 15 E. Florin, R. Kjellander and J. C. Eriksson, *J. Chem. Soc., Faraday Trans. 1*, 1984, **80**, 2889.
- 16 J. R. C. van der Maarel, D. Lankhorst, J. de Bleijser and J. C. Leyte, *J. Phys. Chem.*, 1986, **90**, 1470.
- 17 C. Chachaty and J. P. Quaegebeur, *Mol. Phys.*, 1984, **52**, 1081.
- 18 B. Halle and H. Wennerström, *J. Chem. Phys.*, 1983, **87**, 2336.
- 19 C. W. R. Mulder, J. Schrieffer and J. C. Leyte, *J. Phys. Chem.*, 1983, **87**, 2336.
- 20 B. Benko, V. Buljan and S. Vuk Pavlovic, *J. Phys. Chem.*, 1980, **84**, 913.
- 21 S. Marcelja, D. J. Mitchell, B. W. Ninkam and M. J. Sculley, *J. Chem. Soc., Faraday Trans. 2*, 1977, **73**, 630.
- 22 A. Geiger, A. Rahman and F. H. Stillinger, *J. Chem. Phys.*, 1979, **70**, 263.
- 23 R. Kjellander and S. Marcelja, *Chem. Phys. Lett.*, 1985, **120**, 393.
- 24 D. E. Woessner, *J. Magn. Reson.*, 1980, **39**, 297.
- 25 D. A. Zichi and P. J. Rossky, *J. Chem. Phys.*, 1986, **84**, 2814.
- 26 H. G. Hertz and C. Rädle, *Ber. Bunsenges. Phys. Chem.*, 1973, **77**, 521.
- 27 J. Jen, *J. Magn. Reson.*, 1978, **30**, 111.
- 28 D. Lankhorst, J. Schrieffer and J. C. Leyte, *J. Magn. Reson.*, 1983, **51**, 430.
- 29 D. L. Turner, *Mol. Phys.*, 1980, **40**, 949.
- 30 L. Piculell and B. Halle, *J. Chem. Soc., Faraday Trans. 1*, 1986, **82**, 401.
- 31 J. R. C. van der Maarel, D. Lankhorst, J. de Bleijser and J. C. Leyte, to be published.

Paper 7/417; Received 5th March, 1987